4.6. Cooper, G. E. and R. P. Harper. "The Use of Pilot Rating in the Evaluation of Aircraft Handling Qualities." NASA TN D-5153, 1969.
4.7. Kawamura, R. and Aihara, Y. (Editors), *Fluid Dynamics of High Angle of Attack*, Springer-Verlag, New York, NY, 1993.
4.8. Nelson, R. C. "The Role of Flow Visualization in the Study of High-Angle-of-Attack Aerodynamics." *Tactual Missle Aerodyanics*, Volume 104 of the Progress in Astronautics and Aeronautics Series, American Institute of Aeronautics and Astronautics, New York, NY, 1986.

CHAPTER 5

# Lateral Motion (Stick Fixed)

*"Dutch Roll is a complex oscillating motion of an aircraft involving rolling, yawing and sideslipping. So named for the resemblance to the characteristic rhythm of an ice skater."*

F. D. Adams, *Aeronautical Dictionary* [5.1]

## 5.1 INTRODUCTION

The stick fixed lateral motion of an airplane disturbed from its equilibrium state is a complicated combination of rolling, yawing, and sideslipping motions. As was shown in Chapter 2, an airplane produces both yawing and rolling moments due to the sideslip angle. This interaction between the roll and the yaw produces the coupled motion. Three potential lateral dynamic instabilities are of interest to the airplane designer: directional divergence, spiral divergence, and the so-called Dutch roll oscillation.

Directional divergence can occur when the airplane lacks directional or weathercock stability. If disturbed from its equilibrium state such an airplane will tend to rotate to ever-increasing angles of sideslip. Owing to the side force acting on the airplane, it will fly a curved path at large sideslip angles. For an airplane that has lateral static stability (i.e., dihedral effect) the motion can occur with no significant change in bank angle. Obviously, such a motion cannot be tolerated and readily can be avoided by proper design of the vertical tail surface to ensure directional stability.

Spiral divergence is a nonoscillatory divergent motion that can occur when directional stability is large and lateral stability is small. When disturbed from equilibrium, the airplane enters a gradual spiraling motion. The spiral becomes tighter and steeper as time proceeds and can result in a high-speed spiral dive if corrective action is not taken. This motion normally occurs so gradually that the pilot unconsciously corrects for it.

The Dutch roll oscillation is a coupled lateral-directional oscillation that can be quite objectionable to pilots and passengers. The motion is characterized by a combination of rolling and yawing oscillations that have the same frequency but are out of phase with each other. The period can be on the order of 3 to 15 seconds, so that if the amplitude is appreciable the motion can be very annoying.

Before analyzing the complete set of lateral equations we shall examine several motions with a single degree of freedom. The purpose of examining the single degree of freedom equations is to gain an appreciation of the more complicated motion comprising the stick fixed lateral motion of an airplane.

## 5.2 PURE ROLLING MOTION

A wind-tunnel model free to roll about its $x$ axis is shown in Figure 5.1. The equation of motion for this example of a pure rolling motion is

$$\sum \text{Rolling moments} = I_x \ddot{\phi} \tag{5.1}$$

or

$$\frac{\partial L}{\partial \delta_a} \Delta\delta_a + \frac{\partial L}{\partial p} \Delta p = I_x \Delta\ddot{\phi} \tag{5.2}$$

where $(\partial L/\partial \delta_a)\ \Delta\delta_a$ is the roll moment due to the deflection of the ailerons and $(\partial L/\partial p)\ \Delta p$ is the roll-damping moment. Methods for estimating these derivatives were presented in Chapters 2 and 3. The roll angle $\phi$ is the angle between $z_b$ of the body axes and $z_f$ of the fixed axis system. The roll rate $\Delta p$ is equal to $\Delta\dot{\phi}$, which will allow us to rewrite Equation (5.2) as follows:

$$\tau\, \Delta\dot{p} + \Delta p = -\frac{L_{\delta a}\, \Delta\delta_a}{L_p} \tag{5.3}$$

Here $\tau$, $L_p$, and $L_{\delta a}$ are defined as follows:

$$\tau = -\frac{1}{L_p} \quad \text{and} \quad L_p = \frac{\partial L/\partial p}{I_x} \quad L_{\delta a} = \frac{\partial L/\partial \delta_a}{I_x} \tag{5.4}$$

The parameter $\tau$ is referred to as the time constant of the system. The time constant tells us how fast our system approaches a new steady-state condition after being disturbed. If the time constant is small, the system will respond very rapidly; if the time constant is large, the system will respond very slowly.

The solution to Equation (5.3) for a step change in the aileron angle is

$$\Delta p(t) = -\frac{L_{\delta a}}{L_p}(1 - e^{-t/\tau})\ \Delta\delta_a \tag{5.5}$$

Recall that $C_{l_p}$ is negative; therefore, the time constant will be positive. The roll rate time history for this example will be similar to that shown in Figure 5.2. The steady-state roll rate can be obtained from Equation (5.5), by assuming that time $t$ is large enough that $e^{-t/\tau}$ is essentially 0:

$$p_{ss} = \frac{-L_{\delta a}}{L_p}\, \Delta\delta_a \tag{5.6}$$

$$p_{ss} = \frac{-C_{l_{\delta a}} QSb/I_x}{C_{l_p}(b/2u_0)QSb/I_x}\, \Delta\delta_a \tag{5.7}$$

$$\frac{p_{ss} b}{2u_0} = -\frac{C_{l_{\delta a}}}{C_{l_p}}\, \Delta\delta_a$$



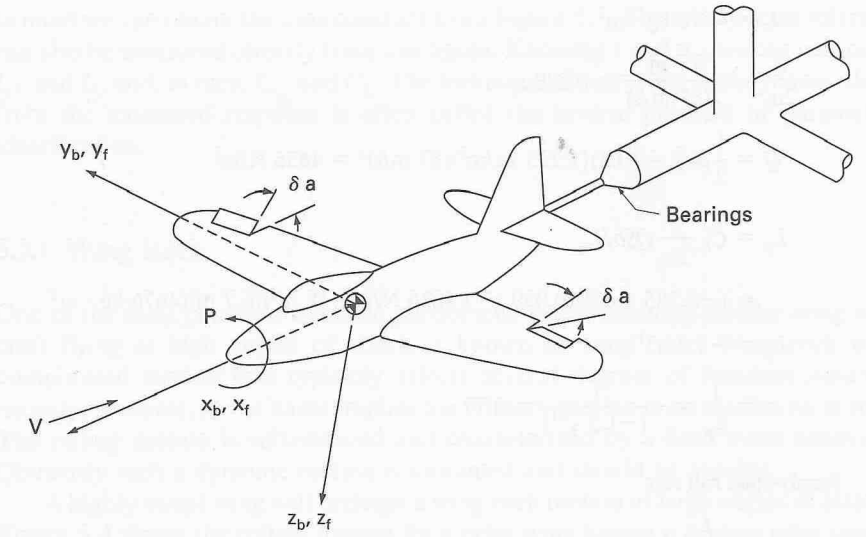


**FIGURE 5.1**
Wind-tunnel model constrained to a pure rolling motion.

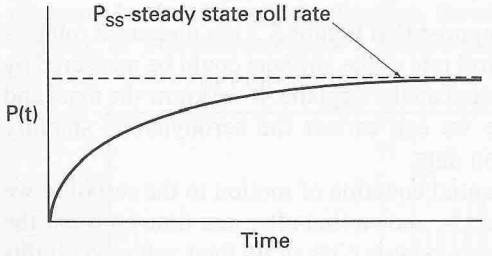


**FIGURE 5.2**
Typical roll response due to aileron deflection.

The term $(p_{ss}b/2u_0)$ for full aileron deflection can be used for sizing the aileron. The minimum requirement for this ratio is a function of the class of airplane under consideration:

Cargo or transport airplanes: $pb/2u_0 = 0.07$
Fighter airplanes: $pb/2u_0 = 0.09$

**EXAMPLE PROBLEM 5.1.** Calculate the roll response of the F104A to a 5° step change in aileron deflection. Assume the airplane is flying at sea level with a velocity of 87 m/s. The F104A has the following aerodynamic and geometric characteristics:

$C_{l_p} = -0.285\ \text{rad}^{-1}$ $\quad S = 18\ \text{m}^2$

$C_{l_{\delta_a}} = 0.039\ \text{rad}^{-1}$ $\quad b = 6.7\ \text{m}$

$$I_x = 4676 \text{ kg} \cdot \text{m}^2$$

$$\frac{b}{2u_0} = \frac{6.7 \text{ m}}{2(87 \text{ m/s})} = 0.039 \text{ s}$$

$$Q = \frac{1}{2}\rho u_0^2 = (0.5)(1.225 \text{ kg/m}^3)(87 \text{ m/s})^2 = 4636 \text{ N/m}^2$$

$$L_p = C_{l_p}\frac{b}{2u_0}QSb/I_x$$

$$= (-0.285 \text{ rad}^{-1})(0.039 \text{ s}^{-1})(4636 \text{ N/m}^2)(18 \text{ m}^2)(6.7 \text{ m})(4676 \text{ kg} \cdot \text{m}^2)$$

$$L_p = -1.3(\text{s}^{-1})$$

$$\tau = \frac{1}{L_p} = -\frac{1}{(-1.3 \text{ s}^{-1})} = 0.77 \text{ s}$$

**Steady-state roll rate**

$$p_{ss} = -\frac{L_{\delta_a}}{L_p}\Delta\delta_a$$

$$L_{\delta_a} = C_{l_{\delta_a}}QSb/I_x$$

$$L_{\delta_a} = (0.039 \text{ rad}^{-1})(4636 \text{ N/m}^2)(18 \text{ m}^2)(6.7 \text{ m})/(4676 \text{ kg} \cdot \text{m}^2) = 4.66 \text{ (s}^{-2})$$

$$p_{ss} = -(4.661 \text{ s}^{-2})(5 \text{ deg})/[(-1.3 \text{ s}^{-1})(57.3 \text{ deg/rad})] = 0.31 \text{ rad/s}$$

Figure 5.3 is a plot of the roll rate time history for a step change in aileron deflection.

Let us reconsider this problem. Suppose that Figure 5.3 is a measured roll rate instead of a calculated response. The roll rate of the airplane could be measured by means of a rate gyro appropriately located on the airplane. If we know the mass and geometric properties of the airplane we can extract the aerodynamic stability coefficients from the measured motion data.

If we fit the solution to the differential equation of motion to the response we can obtain values for $C_{l_{\delta_a}}$ and $C_{l_p}$. It can be shown that after one time constant the response of a first-order system to a step input is 63% of its final value. With this

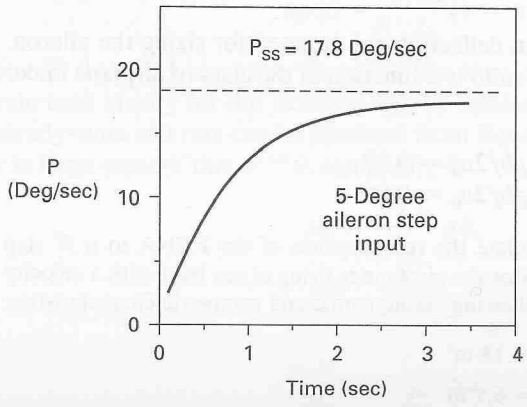


**FIGURE 5.3**
Roll time history of an F104A to a 5° step change in aileron deflection.



in mind we can obtain the time constant from Figure 5.3. The steady-state roll rate can also be measured directly from this figure. Knowing $\tau$ and $p_{ss}$, we can compute $L_{\delta_a}$ and $L_p$ and, in turn, $C_{l_{\delta_a}}$ and $C_{l_p}$. The technique of extracting aerodynamic data from the measured response is often called the inverse problem or parameter identification.

### 5.2.1 Wing Rock

One of the most common dynamic phenomena experienced by slender-wing aircraft flying at high angles of attack is known as wing rock. Wing rock is a complicated motion that typically affects several degrees of freedom simultaneously; however, as the name implies the primary motion is an oscillation in roll. The rolling motion is self-induced and characterized by a limit cycle behavior. Obviously such a dynamic motion is unwanted and should be avoided.

A highly swept wing will undergo a wing rock motion at large angles of attack. Figure 5.4 shows the rolling motion for a delta wing having a leading edge sweep of 80° (from [5.2] and [5.3]). The wing was mounted on an air bearing system that permitted only a free to roll motion. The model was released with initial conditions $\phi = 0$ and $\dot{\phi} = 0$. The model is unstable in a roll: The motion begins to build up until it reaches some maximum amplitude at which time it continues to repeat the motion. This type of motion is called a limit cycle oscillation. The limit cycle motion clearly is indicated when the response data is plotted in a phase plane diagram. In the phase plane diagram, the amplitude, $\phi$, is plotted versus the roll velocity, $\dot{\phi}$. The data in Figure 5.4 when plotted in the phase plane is as shown on

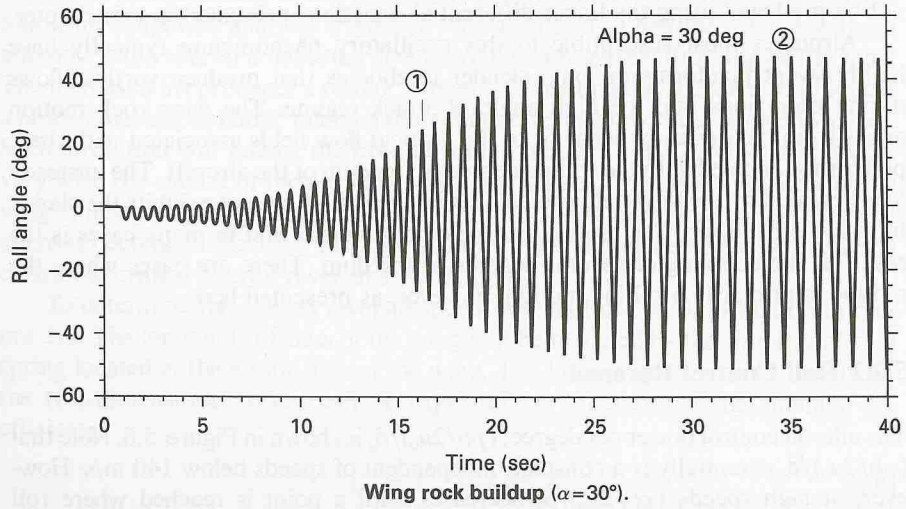


**FIGURE 5.4**
Wing rock motion of a flat plate delta wing.
Leading edge sweep angle of 80° and $\alpha = 30°$

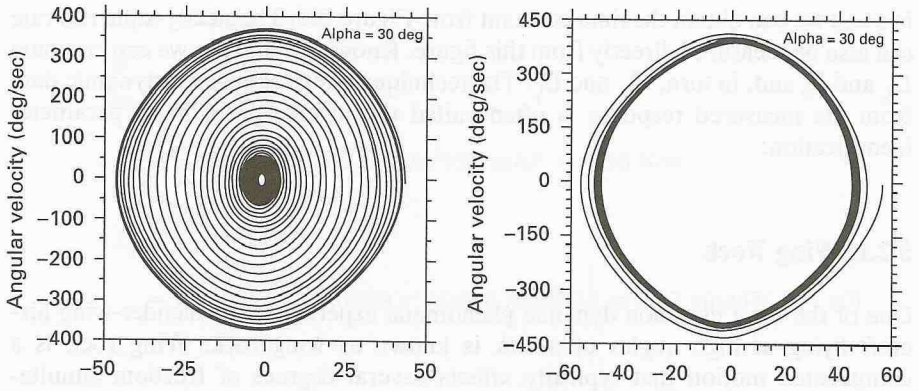


**Phase plane of wing rock buildup ($\alpha = 30°$).** **Phase plane of wing rock for $\phi_0 = 55°$ ($\alpha = 30°$).**

**FIGURE 5.5**
Phase plane plots of the wing rock motion of a delta wing.

the left side of Figure 5.5. The motion is observed to spiral out to the limit cycle. If the initial conditions on release were any combination on $\phi$ and $\dot{\phi}$ within the limit cycle boundary the motion would still spiral out the limit cycle boundary. On the other hand if the initial conditions were outside the limit cycle boundary the motion would spiral into the limit cycle as illustrated on the right side of Figure 5.5. The limit cycle motion is due to the nonlinear aerodynamic characteristics of a slender delta wing at large angles of attack. Because the aerodynamics are nonlinear, the equation of motion also will be nonlinear. This type of motion can not be predicted using the linear differential equations presented in this chapter.

Airplanes most susceptible to this oscillatory phenomenon typically have highly swept planforms or long, slender forebodies that produce vortical flows during excursions into the high angle-of-attack regime. The wing rock motion arises from the unsteady behavior of the vortical flow fields associated with these planforms, coupled with the rolling degree of freedom of the aircraft. The unsteady loads created by the flow field produce a rolling oscillation that exhibits the classic limit cycle behavior. The motion can be quite complex and in many cases is the result of the coupling of several degrees of freedom. There are cases where the motion is primarily a rolling motion, however, as presented here.

### 5.2.2 Roll Control Reversal

The aileron control power per degree, $(pb/2u_0)/\delta_a$ is shown in Figure 5.6. Note that $(pb/2u_0)/\delta_a$ essentially is a constant, independent of speeds below 140 m/s. However, at high speeds $(pb/2u_0)/\delta_a$ decreases until a point is reached where roll control is lost. The point at which $(pb/2u_0)/\delta_a = 0$ is called the aileron reversal speed. The loss and ultimate reversal of aileron control is due to the elasticity of the wing.



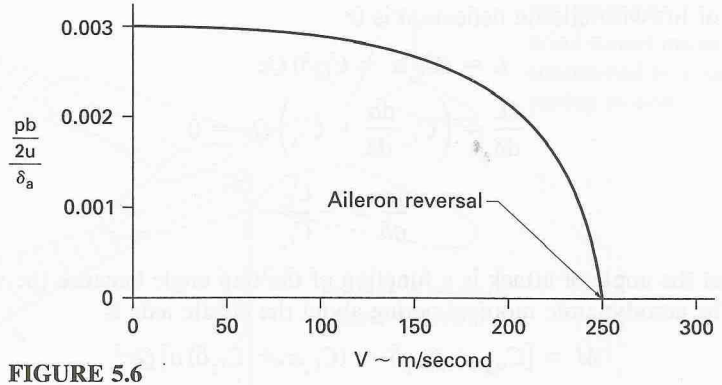


**FIGURE 5.6**
Aileron control power per degree versus flight velocity.

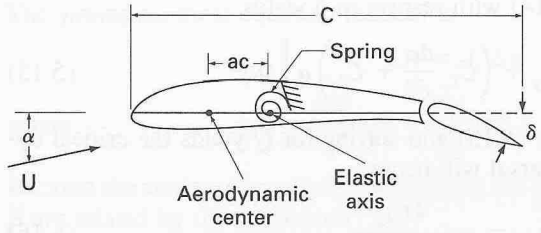


**FIGURE 5.7**
Two-dimensional wing and aileron.

Some understanding of this aeroelastic phenomenon can be obtained from the following simplified analysis. Figure 5.7 shows a two-dimensional wing with an aileron. As the aileron is deflected downward it increases the lift acting on the wing. The increased lift produces a rolling moment. Deflecting the aileron also produces a nose-down aerodynamic pitching moment that tends to twist the wing downward. Such a rotation will reduce the lift and rolling moment. The aerodynamic forces vary with the square of the airplane's velocity whereas the elastic stiffness of the wing is independent of the flight speed. Thus, the wing may twist enough that the ailerons become ineffective. The speed at which the ailerons become ineffective is called the critical aileron reversal speed.

To determine the aileron reversal speed, we shall use the information in Figure 5.7. The torsional stiffness of the wing will be modeled by the simple torsional spring located at the elastic axis of the wing. The lift and moment coefficients for the two-dimensional airfoil can be expressed as functions of the stability coefficients:

$$C_\ell = C_{\ell_\alpha}\alpha + C_{\ell_\delta}\delta \tag{5.8}$$

$$C_m = C_{m_{ac}} + C_{m_\delta}\delta \tag{5.9}$$

where $\delta$ is the flap angle; that is, aileron. Aileron reversal occurs when the rate of

change of lift with aileron deflection is 0:

$$L = (C_{\ell_\alpha}\alpha + C_{\ell_\delta}\delta)\,Qc \tag{5.10}$$

$$\frac{dL}{d\delta} = \left(C_{\ell_\alpha}\frac{d\alpha}{d\delta} + C_{\ell_\delta}\right)Qc = 0 \tag{5.11}$$

or

$$\frac{d\alpha}{d\delta} = -\frac{C_{\ell_\delta}}{C_{\ell_\alpha}} \tag{5.12}$$

Note that the angle of attack is a function of the flap angle because the wing can twist. The aerodynamic moment acting about the elastic axis is

$$M = [C_{m_{ac}} + C_{m_\delta}\delta + (C_{\ell_\alpha}\alpha + C_{\ell_\delta}\delta)\,a]\,Qc^2 \tag{5.13}$$

This moment is balanced by the torsional moment to the wing:

$$k\alpha = [C_{m_{ac}} + C_{m_\delta}\delta + (C_{\ell_\alpha}\alpha + C_{\ell_\delta}\delta)\,a]\,Qc^2 \tag{5.14}$$

where $k$ is the torsional stiffness of the wing.

Differentiating Equation (5.14) with respect to $\delta$ yields

$$k\frac{d\alpha}{d\delta} = \left[C_{m_\delta} + \left(C_{\ell_\alpha}\frac{d\alpha}{d\delta} + C_{\ell_\delta}\right)a\right]Qc^2 \tag{5.15}$$

Substituting Equation (5.12) into (5.15) and solving for $Q$ yields the critical dynamic pressure when control reversal will occur:

$$Q_{\text{rev}} = -\frac{kC_{\ell_\delta}}{c^2 C_{\ell_\alpha} C_{m_\delta}} \tag{5.16}$$

The reversal speed is given by

$$U_{\text{rev}} = \sqrt{-\frac{2kC_{\ell_\delta}}{\rho c^2 C_{\ell_\alpha} C_{m_\delta}}} \tag{5.17}$$

Note that the reversal speed increases with increasing torsional stiffness and increasing altitude.

## 5.3 PURE YAWING MOTION

As our last example of a motion with a single degree of freedom, we shall examine the motion of an airplane constrained so that it can perform only a simple yawing motion. Figure 5.8 illustrates a wind-tunnel model that can only perform yawing motions. The equation of motion can be written as follows:

$$\sum \text{Yawing moments} = I_z\ddot{\psi} \tag{5.18}$$

The yawing moment $N$ and the yaw angle $\psi$ can be expressed as

$$N = N_0 + \Delta N \qquad \psi = \psi_0 + \Delta\psi \tag{5.19}$$



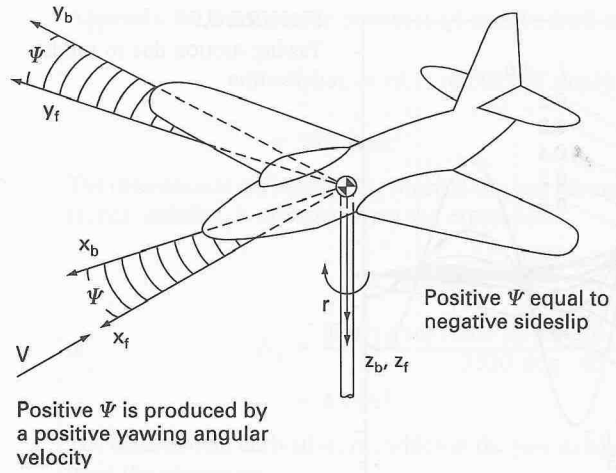


**FIGURE 5.8**
Wind-tunnel model constrained to a pure yawing motion.

The yawing moment equation reduces to

$$\Delta N = I_z\,\Delta\ddot{\psi} \tag{5.20}$$

where

$$\Delta N = \frac{\partial N}{\partial\beta}\Delta\beta + \frac{\delta N}{\delta\dot{\beta}}\Delta\dot{\beta} + \frac{\partial N}{\partial r}\Delta r + \frac{\partial N}{\partial\delta_r}\Delta\delta_r \tag{5.21}$$

Because the center of gravity is constrained, the yaw angle $\psi$ and the sideslip angle $\beta$ are related by the expression

$$\Delta\psi = -\Delta\beta \qquad \Delta\dot{\psi} = -\Delta\dot{\beta} \qquad \Delta\dot{\psi} = \Delta r \tag{5.22}$$

Substituting these relationships into Equation (5.20) and rearranging yields

$$\Delta\ddot{\psi} - (N_r - N_{\dot{\beta}})\,\Delta\dot{\psi} + N_\beta\,\Delta\psi = N_{\delta_r}\,\Delta\delta_r \tag{5.23}$$

where

$$N_r = \frac{\partial N/\partial r}{I_z} \qquad \text{and so forth.}$$

For airplanes, the term $N_{\dot{\beta}}$ usually is negligible and will be eliminated in future expressions.

The characteristic equation for Equation (5.23) is

$$\lambda^2 - N_r\lambda + N_\beta = 0 \tag{5.24}$$

The damping ratio $\zeta$ and the undamped natural frequency $\omega_n$ can be determined directly from Equation (5.24):

$$\omega_n = \sqrt{N_\beta} \tag{5.25}$$

$$\zeta = -\frac{N_r}{2\sqrt{N_\beta}} \tag{5.26}$$

The solution to Equation (5.23) for a step change in the rudder control will result in a damped sinusoidal motion, provided the airplane has sufficient aerodynamic damping. As in the case of the pure pitching we see that the frequency of

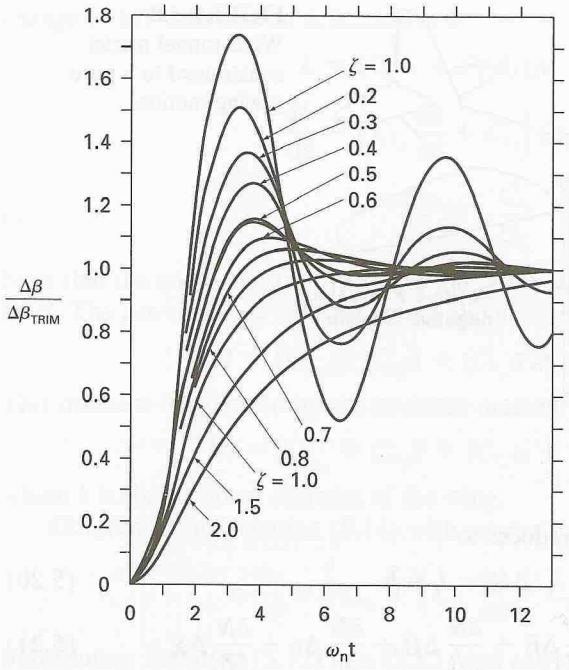


**FIGURE 5.9**
Yawing motion due to rudder deflection.

oscillation is a function of the airplane's static stability (weathercock or directional stability) and the damping ratio is a function of the aerodynamic damping derivative. Figure 5.9 illustrates the yawing motion due to a step change in rudder deflections for different levels of aerodynamic damping.

**EXAMPLE PROBLEM 5.2.** Suppose an airplane is constrained to a pure yawing motion as described in Section 5.3. Using the data for the general aviation airplane in Appendix B, determine the following:

(*a*) The yawing moment equation rewritten in state-space form.
(*b*) The characteristic equation and eigenvalues for the system.
(*c*) The damping ratio, $\zeta$, and undamped natural frequency, $\omega_n$.
(*d*) The response of the airplane to a 5° rudder input. Assume the initial conditions are $\Delta\beta(0) = 0$, $\Delta r(0) = 0$.

***Solution.*** The lateral derivatives can be estimated from the data in Appendix B. For the sea-level flight condition, the weathercock static stability coefficient, $C_{n_\beta}$, the yawing damping coefficient, $C_{n_r}$, and the rudder control power, $C_{n_{\delta_r}}$, have the following numerical values:

$$C_{n_\beta} = 0.071/\text{rad} \qquad C_{n_r} = -0.125/\text{rad}$$
$$C_{n_{\delta_r}} = -0.072/\text{rad}$$

The derivative $C_{n_{\dot\beta}}$ is not included in the table of Appendix B and will be assumed to be 0 for this problem.

For a flight velocity of 176 ft/s, the dimensional derivatives $N_\beta$, $N_r$, and $N_{\delta_r}$ can be estimated from the mass, geometric, and aerodynamic stability coefficient data of



Appendix B. The dynamic pressure, $Q$, is calculated next:

$$Q = \frac{1}{2}\rho u_0^2 = (0.5)\ (0.002378\ \text{slug/ft}^3)\ (176\ \text{ft/s})^2$$
$$= 36.8\ \text{lb/ft}^2$$

The dimensional derivative, $N_\beta$, which is the yaw moment due to the airplane's weathercock stability, is obtained from the expression

$$N_\beta = \frac{C_{n_\beta} QSb}{I_z}$$

or

$$N_\beta = \frac{(0.071/\text{rad})\ (36.8\ \text{lb/ft}^2)\ (184\ \text{ft}^2)\ (33.4\ \text{ft})}{3530\ \text{slug} \cdot \text{ft}^2}$$
$$= 4.55/\text{s}^2$$

The dimensional derivative, $N_r$, which is the yaw damping of the airplane, is obtained from the expression

$$N_r = \frac{C_{n_r}\left(\frac{b}{2u_0}\right) QSb}{I_z}$$
$$= \frac{(-0.125/\text{rad})\ [33.4\ \text{ft}/(2(176\ \text{ft/s}))]\ (36.8\ \text{lb/ft}^2)\ (184\ \text{ft}^2)\ (33.4\ \text{ft})}{3530\ \text{slug} \cdot \text{ft}^2}$$
$$= -0.76/\text{s}$$

The dimensional derivative, $N_{\delta_r}$, the rudder control derivative, is obtained from the expression

$$N_{\delta_r} = \frac{C_{n_{\delta_r}} QSb}{I_z}$$
$$= \frac{(-0.072/\text{rad})\ (36.8\ \text{lb/ft}^2)\ (184\ \text{ft}^2)\ (33.4\ \text{ft})}{3530\ \text{slug} \cdot \text{ft}^2}$$
$$= -4.6/\text{s}^2$$

Substituting the dimensional derivatives into the constrained yawing moment equation (Equation (5.23)) yields

$$\Delta\ddot\psi - (N_r - N_{\dot\beta})\,\Delta\dot\psi + N_\beta\,\Delta\psi = N_{\delta_r}\,\Delta\delta_r$$

where $N_{\dot\beta}$ is assumed to be 0:

$$\Delta\ddot\psi + 0.76\,\Delta\dot\psi + 4.55\,\Delta\psi = -4.6\,\Delta\delta_r$$

This is a second-order differential equation in terms of the dependent variable $\Delta\psi$. The preceding second-order differential equation can be written as a system of two first-order differential equations by defining the system states as $\Delta\psi$ and $\Delta r$. Recall that the time rate of change of the yaw angle is the same as the yaw rate; that is, $\Delta\dot\psi = \Delta r$. Solving the yaw moment equation for the highest order derivative $\Delta\ddot\psi$,

$$\Delta\ddot\psi = -0.76\,\Delta\dot\psi - 4.55\,\Delta\psi - 4.6\,\Delta\delta_r$$

or

$$\Delta\dot r = -0.76\,\Delta r - 4.55\,\Delta\psi - 4.6\,\Delta\delta_r$$

The two state equations are

$$\Delta\dot{\psi} = \Delta r$$

$$\Delta\dot{r} = -0.76\,\Delta r - 4.55\,\Delta\psi - 4.6\,\Delta\delta_r$$

which can be readily arranged in matrix form as

$$\begin{bmatrix}\Delta\dot{\psi}\\ \Delta\dot{r}\end{bmatrix} = \begin{bmatrix}0 & 1\\ -4.55 & -0.76\end{bmatrix}\begin{bmatrix}\Delta\psi\\ \Delta r\end{bmatrix} + \begin{bmatrix}0\\ -4.6\end{bmatrix}\Delta\delta_r$$

or

$$\dot{\mathbf{x}} = \mathbf{A}\mathbf{x} + \mathbf{B}\boldsymbol{\eta}$$

where the state vector, $\mathbf{x} = \begin{bmatrix}\Delta\psi\\ \Delta r\end{bmatrix}$, the control vector is $\Delta\delta_r$, and the **A** and **B** matrices are

$$\mathbf{A} = \begin{bmatrix}0 & 1\\ -4.55 & -0.76\end{bmatrix}$$

$$\mathbf{B} = \begin{bmatrix}0\\ -4.6\end{bmatrix}$$

The characteristic equation for the system is found from the equation

$$|\lambda\mathbf{I} - \mathbf{A}| = 0$$

where on substituting in the **A** matrix yields

$$\left|\lambda\begin{bmatrix}1 & 0\\ 0 & 1\end{bmatrix} - \begin{bmatrix}0 & 1\\ -4.55 & -0.76\end{bmatrix}\right| = 0$$

$$\begin{vmatrix}\lambda & -1\\ 4.55 & \lambda + 0.76\end{vmatrix} = \lambda(\lambda + 0.76) + 4.55 = 0$$

or

$$\lambda^2 + 0.76\lambda + 4.55 = 0$$

The characteristic equation for a second-order system could have been obtained directly from the second-order differential equation.

The eigenvalues of the system are found by obtaining the roots of the characteristic equation. For this example the root or eigenvalues can be shown to be

$$\lambda_{1,2} = -0.38 \pm 2.1\mathrm{i}$$

The eigenvalues are complex; therefore the free response motion will be a damped sinusoidal oscillation. The motion is damped because the real part of the eigenvalue is negative.

The damping ratio, $\zeta$, and the undamped natural frequency can be estimated from Equations (5.25) and (5.26):

$$\omega_n = \sqrt{N_\beta} = \sqrt{4.55/\mathrm{s}^2} = 2.13\ \mathrm{rad/s}$$

and

$$\zeta = -\frac{N_r}{2\sqrt{N_\beta}} = -\frac{(0.76/\mathrm{s})}{2(2.13\ \mathrm{rad/s})} = 0.178$$



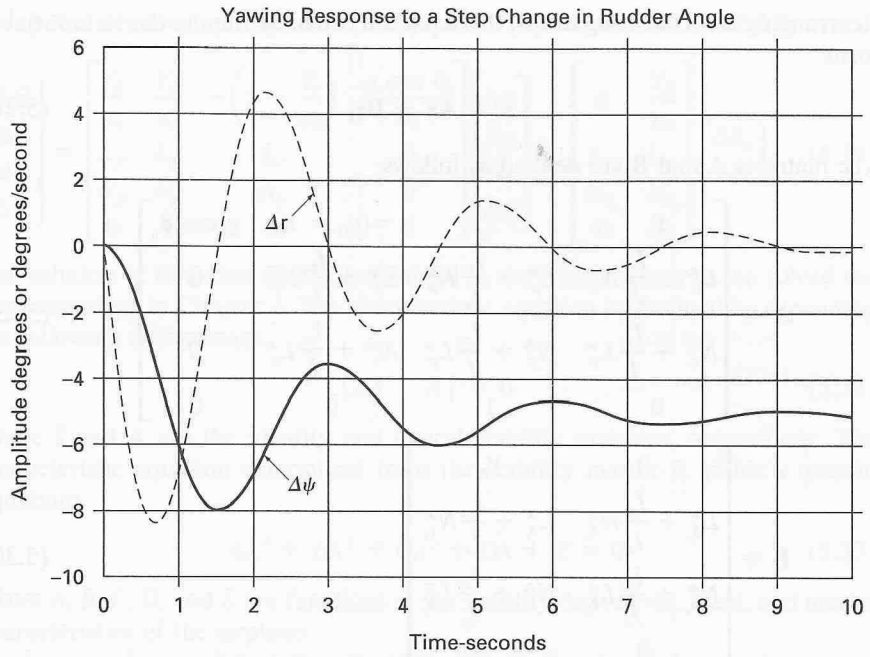


**FIGURE 5.10**
Yawing motion response to a 5° step input in the rudder angle.

Finally the response of the airplane to a 5° step input in the rudder is shown in Figure 5.10. The change in both heading angle $\Delta\psi$ and the yaw rate $\Delta r$ are presented as a function of time. The response was determined using MATLAB.

## 5.4 LATERAL-DIRECTIONAL EQUATIONS OF MOTION

The lateral-directional equations of motion consist of the side force, rolling moment, and yawing moment equations of motion. The lateral equations of motion can be rearranged into the state-space form in the following manner. We start with a lateral set of Equations (5.27):

$$\left(\frac{\mathrm{d}}{\mathrm{d}t} - Y_v\right)\Delta v - Y_p\,\Delta p + (u_0 - Y_r)\,\Delta r - g\cos\theta_0\,\Delta\phi = Y_{\delta_r}\,\Delta\delta_r$$

$$-L_v\,\Delta v + \left(\frac{\mathrm{d}}{\mathrm{d}t} - L_p\right)\Delta p - \left(\frac{I_{xz}}{I_x}\frac{\mathrm{d}}{\mathrm{d}t} + L_r\right)\Delta r = L_{\delta_a}\,\Delta\delta_a + L_{\delta_r}\,\Delta\delta_r \qquad (5.27)$$

$$-N_v\,\Delta v - \left(\frac{I_{xz}}{I_z}\frac{\mathrm{d}}{\mathrm{d}t} + N_p\right)\Delta p + \left(\frac{\mathrm{d}}{\mathrm{d}t} - N_r\right)\Delta r = N_{\delta_a}\,\Delta\delta_a + N_{\delta_r}\,\Delta\delta_r$$

Rearranging and collecting terms, this equation can be written in the state variable form:

$$\dot{\mathbf{x}} = \mathbf{A}\mathbf{x} + \mathbf{B}\boldsymbol{\eta} \tag{5.28}$$

The matrices **A** and **B** are defined as follows:

$$\mathbf{A} = \begin{bmatrix} Y_v & Y_p & -(u_0 - Y_r) & g\cos\theta_0 \\ L_v^* + \frac{I_{xz}}{I_x}N_v^* & L_p^* + \frac{I_{xz}}{I_x}N_p^* & L_r^* + \frac{I_{xz}}{I_x}N_r^* & 0 \\ N_v^* + \frac{I_{xz}}{I_z}L_v^* & N_p^* + \frac{I_{xz}}{I_z}L_p^* & N_r^* + \frac{I_{xz}}{I_z}L_r^* & 0 \\ 0 & 1 & 0 & 0 \end{bmatrix} \tag{5.29}$$

$$\mathbf{B} = \begin{bmatrix} 0 & Y_{\delta_r} \\ L_{\delta_a}^* + \frac{I_{xz}}{I_x}N_{\delta_a}^* & L_{\delta_r}^* + \frac{I_{xz}}{I_x}N_{\delta_r}^* \\ N_{\delta_a}^* + \frac{I_{xz}}{I_z}L_{\delta_a}^* & N_{\delta_r}^* + \frac{I_{xz}}{I_z}L_{\delta_r}^* \\ 0 & 0 \end{bmatrix} \tag{5.30}$$

$$\mathbf{x} = \begin{bmatrix} \Delta v \\ \Delta p \\ \Delta r \\ \Delta\phi \end{bmatrix} \quad \text{and} \quad \boldsymbol{\eta} = \begin{bmatrix} \Delta\delta_a \\ \Delta\delta_r \end{bmatrix} \tag{5.31}$$

The starred derivatives are defined as follows:

$$L_v^* = \frac{L_v}{[1 - (I_{xz}^2/(I_x I_z))]} \qquad N_v^* = \frac{N_v}{[1 - (I_{xz}^2/(I_x I_z))]} \qquad \text{and the like.} \tag{5.32}$$

If the product of intertia $I_{xz} = 0$, the equations of motion reduce to the following form:

$$\begin{bmatrix} \Delta\dot{v} \\ \Delta\dot{p} \\ \Delta\dot{r} \\ \Delta\dot{\phi} \end{bmatrix} = \begin{bmatrix} Y_v & Y_p & -(u_0 - Y_r) & g\cos\theta_0 \\ L_v & L_p & L_r & 0 \\ N_v & N_p & N_r & 0 \\ 0 & 1 & 0 & 0 \end{bmatrix} \begin{bmatrix} \Delta v \\ \Delta p \\ \Delta r \\ \Delta\phi \end{bmatrix} + \begin{bmatrix} 0 & Y_{\delta_r} \\ L_{\delta_a} & L_{\delta_r} \\ N_{\delta_a} & N_{\delta_r} \\ 0 & 0 \end{bmatrix} \begin{bmatrix} \Delta\delta_a \\ \Delta\delta_r \end{bmatrix} \tag{5.33}$$

It sometimes is convenient to use the sideslip angle $\Delta\beta$ instead of the side velocity $\Delta v$. These two quantities are related to each other in the following way:

$$\Delta\beta \approx \tan^{-1}\frac{\Delta v}{u_0} = \frac{\Delta v}{u_0} \tag{5.34}$$



Using this relationship, Equation (5.33) can be expressed in terms of $\Delta\beta$:

$$\begin{bmatrix} \Delta\dot{\beta} \\ \Delta\dot{p} \\ \Delta\dot{r} \\ \Delta\dot{\phi} \end{bmatrix} = \begin{bmatrix} \frac{Y_\beta}{u_0} & \frac{Y_p}{u_0} & -\left(1 - \frac{Y_r}{u_0}\right) & \frac{g\cos\theta_0}{u_0} \\ L_\beta & L_p & L_r & 0 \\ N_\beta & N_p & N_r & 0 \\ 0 & 1 & 0 & 0 \end{bmatrix} \begin{bmatrix} \Delta\beta \\ \Delta p \\ \Delta r \\ \Delta\phi \end{bmatrix} + \begin{bmatrix} 0 & \frac{Y_{\delta_r}}{u_0} \\ L_{\delta_a} & L_{\delta_r} \\ N_{\delta_a} & N_{\delta_r} \\ 0 & 0 \end{bmatrix} \begin{bmatrix} \Delta\delta_a \\ \Delta\delta_r \end{bmatrix} \tag{5.35}$$

The solution of Equation (5.35) is obtained in the same manner as we solved the state equations in Chapter 4. The characteristic equation is obtained by expanding the following determinant:

$$|\lambda_r\mathbf{I} - \mathbf{A}| = 0 \tag{5.36}$$

where **I** and **A** are the identity and lateral stability matrices, respectively. The characteristic equation determined from the stability matrix **A** yields a quartic equation:

$$A\lambda^4 + B\lambda^3 + C\lambda^2 + D\lambda + E = 0 \tag{5.37}$$

where $A$, $B$, $C$, $D$, and $E$ are functions of the stability derivatives, mass, and inertia characteristics of the airplane.

In general, we will find the roots to the lateral-directional characteristic equation to be composed of two real roots and a pair of complex roots. The roots will be such that the airplane response can be characterized by the following motions:

1. A slowly convergent or divergent motion, called the spiral mode.
2. A highly convergent motion, called the rolling mode.
3. A lightly damped oscillatory motion having a low frequency, called the Dutch roll mode.

Figures 5.11, 5.12, and 5.13 illustrate the spiral, roll, and Dutch roll motions. An unstable spiral mode results in a turning flight trajectory. The airplane's bank angle increases slowly and it flies in an ever-tightening spiral dive. The rolling motion usually is highly damped and will reach a steady state in a very short time. The combination of the yawing and rolling oscillations is called the Dutch roll motion because it reminded someone of the weaving motion of a Dutch ice skater.

### 5.4.1 Spiral Approximation

As indicated in Figure 5.11 the spiral mode is characterized by changes in the bank angle $\phi$ and the heading angle $\psi$. The sideslip angle usually is quite small but cannot be neglected because the aerodynamic moments do not depend on the roll angle $\phi$ or the heading angle $\psi$ but on the sideslip angle $\beta$, roll rate $p$, and yawing rate $r$.

The aerodynamic contributions due to $\beta$ and $r$ usually are on the same order of magnitude. Therefore, to obtain an approximation of the spiral mode we shall

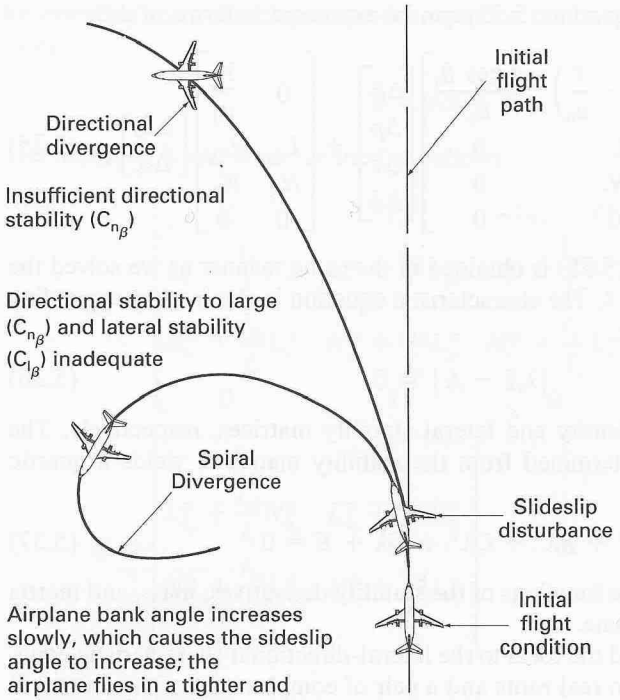


**FIGURE 5.11**
The spiral motion.

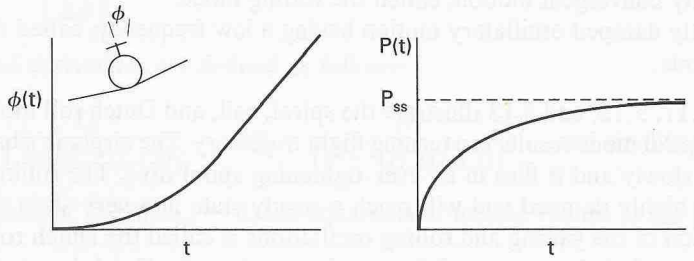


**FIGURE 5.12**
The roll motion.

neglect the side force equation and $\Delta\phi$. With these assumptions, the equations of motion for the approximation can be obtained from Equation (5.35):

$$L_\beta \Delta\beta + L_r \Delta r = 0 \tag{5.38}$$

$$\Delta\dot{r} = N_\beta \Delta\beta + N_r \Delta r \tag{5.39}$$

or

$$\Delta\dot{r} + \frac{L_r N_\beta - L_\beta N_r}{L_\beta} \Delta r = 0 \tag{5.40}$$



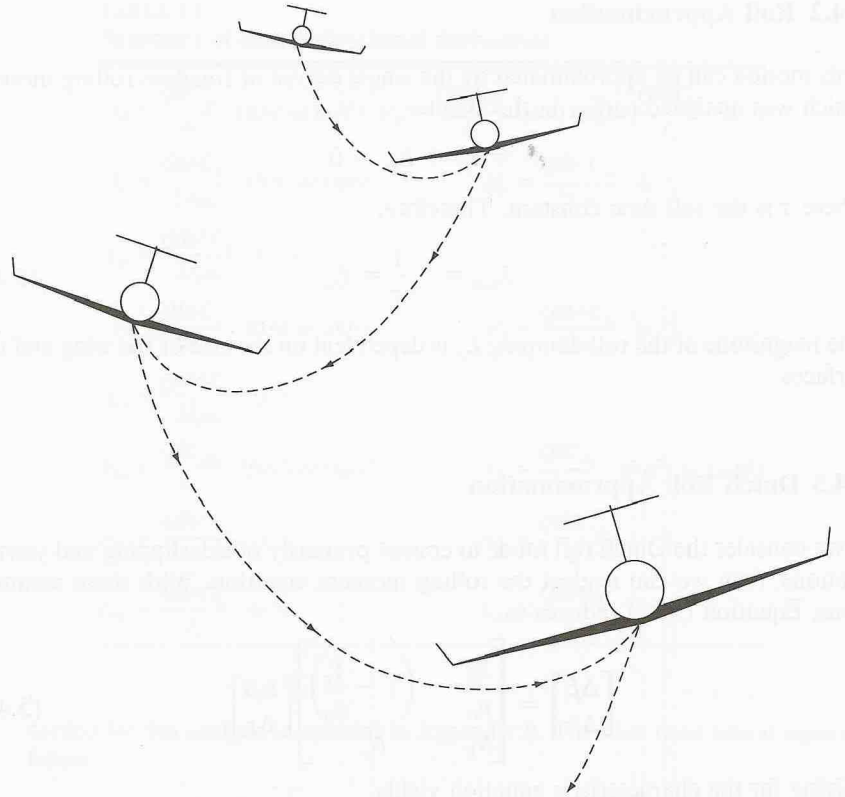

**FIGURE 5.13**
The Dutch roll motion.

The characteristic root for this equation is

$$\lambda_{\text{spiral}} = \frac{L_\beta N_r - L_r N_\beta}{L_\beta} \tag{5.41}$$

The stability derivatives $L_\beta$ (dihedral effect) and $N_r$ (yaw rate damping) usually are negative quantities. On the other hand, $N_\beta$ (directional stability) and $L_r$ (roll moment due to yaw rate) generally are positive quantities. If the derivatives have the usual sign, then the condition for a stable spiral model is

$$L_\beta N_r - N_\beta L_r > 0 \tag{5.42}$$

or

$$L_\beta N_r > N_\beta L_r \tag{5.43}$$

Increasing the dihedral effect $L_\beta$ or the yaw damping or both can make the spiral mode stable.

### 5.4.2 Roll Approximation

This motion can be approximated by the single degree of freedom rolling motion, which was analyzed earlier in the chapter:

$$\tau \Delta\dot{p} + \Delta p = 0$$

where $\tau$ is the roll time constant. Therefore,

$$\lambda_{\text{roll}} = -\frac{1}{\tau} = L_p \tag{5.44}$$

The magnitude of the roll damping $L_p$ is dependent on the size of the wing and tail surfaces.

### 5.4.3 Dutch Roll Approximation

If we consider the Dutch roll mode to consist primarily of sideslipping and yawing motions, then we can neglect the rolling moment equation. With these assumptions, Equation (5.35) reduces to

$$\begin{bmatrix} \Delta\dot{\beta} \\ \Delta\dot{r} \end{bmatrix} = \begin{bmatrix} \frac{Y_\beta}{u_0} & -\left(1 - \frac{Y_r}{u_0}\right) \\ N_\beta & N_r \end{bmatrix} \begin{bmatrix} \Delta\beta \\ \Delta r \end{bmatrix} \tag{5.45}$$

Solving for the characteristic equation yields

$$\lambda^2 - \left(\frac{Y_\beta + u_0 N_r}{u_0}\right)\lambda + \frac{Y_\beta N_r - N_\beta Y_r + u_0 N_\beta}{u_0} = 0 \tag{5.46}$$

From this expression we can determine the undamped natural frequency and the damping ratio as follows:

$$\omega_{n_{\text{DR}}} = \sqrt{\frac{Y_\beta N_r - N_\beta Y_r + u_0 N_\beta}{u_0}} \tag{5.47}$$

$$\zeta_{\text{DR}} = -\frac{1}{2\omega_{n_{\text{DR}}}}\left(\frac{Y_\beta + u_0 N_r}{u_0}\right) \tag{5.48}$$

The approximations developed in this section give, at best, only a rough estimate of the spiral and Dutch roll modes. The approximate formulas should, therefore, be used with caution. The reason for the poor agreement between the approximate and exact solutions is that the Dutch roll motion is truly a three-degree-of-freedom motion with strong coupling between the equations.

**EXAMPLE PROBLEM 5.3.** Find the lateral eigenvalues of the general aviation airplane described in Chapter 4 and compare these results with the answers obtained using the lateral approximations. A summary of the aerodynamic and geometric data



**TABLE 5.1**
**Summary of lateral directional derivatives**

$Y_\beta = \frac{QSC_{y_\beta}}{m}$ (ft/s² or m/s²) $N_\beta = \frac{QSbC_{n_\beta}}{I_z}$ ($s^{-2}$) $L_\beta = \frac{QSbC_{l_\beta}}{I_x}$ ($s^{-2}$)

$Y_p = \frac{QSbC_{y_p}}{2mu_0}$ (ft/s) or (m/s) $N_p = \frac{QSb^2C_{n_p}}{2I_zu_0}$ ($s^{-1}$)

$L_p = \frac{QSb^2C_{l_p}}{2I_xu_0}$ ($s^{-1}$)

$Y_r = \frac{QSbC_{y_r}}{2mu_0}$ (ft/s) or (m/s) $N_r = \frac{QSb^2C_{n_r}}{2I_zu_0}$ ($s^{-1}$)

$L_r = \frac{QSb^2C_{l_r}}{2I_xu_0}$ ($s^{-1}$)

$Y_{\delta a} = \frac{QSC_{y_{\delta a}}}{m}$ (ft/s²) or (m/s²) $Y_{\delta r} = \frac{QSC_{y_{\delta r}}}{m}$ (ft/s²) or (m/s²)

$N_{\delta a} = \frac{QSbC_{n_{\delta a}}}{I_z}$ ($s^{-2}$) $N_{\delta r} = \frac{QSbC_{n_{\delta r}}}{I_z}$ ($s^{-2}$)

$L_{\delta a} = \frac{QSbC_{l_{\delta a}}}{I_x}$ ($s^{-2}$) $L_{\delta r} = \frac{QSbC_{l_{\delta r}}}{I_x}$ ($s^{-2}$)

needed for this analysis is included in Appendix B. The stick fixed lateral equations follow:

$$\begin{bmatrix} \Delta\dot{\beta} \\ \Delta\dot{p} \\ \Delta\dot{r} \\ \Delta\dot{\phi} \end{bmatrix} = \begin{bmatrix} \frac{Y_\beta}{u_0} & \frac{Y_p}{u_0} & -\left(1 - \frac{Y_r}{u_0}\right) & \frac{g}{u_0}\cos\theta_0 \\ L_\beta & L_p & L_r & 0 \\ N_\beta & N_p & N_r & 0 \\ 0 & 1 & 0 & 0 \end{bmatrix} \begin{bmatrix} \Delta\beta \\ \Delta p \\ \Delta r \\ \Delta\phi \end{bmatrix}$$

Before we can determine the eigenvalues of the stability matrix **A**, we first must calculate the lateral stability derivatives. Table 5.1 is a summary of the lateral stability derivative definitions and Table 5.2 gives a summary of the values of these derivatives for the general aviation airplane.

Substituting the lateral stability derivatives into the stick fixed lateral equations yields

$$\dot{\mathbf{x}} = \mathbf{A}\mathbf{x}$$

or

$$\begin{bmatrix} \Delta\dot{\beta} \\ \Delta\dot{p} \\ \Delta\dot{r} \\ \Delta\dot{\phi} \end{bmatrix} = \begin{bmatrix} -0.254 & 0 & -1.0 & 0.182 \\ -16.02 & -8.40 & 2.19 & 0 \\ 4.488 & -0.350 & -0.760 & 0 \\ 0 & 1 & 0 & 0 \end{bmatrix} \begin{bmatrix} \Delta\beta \\ \Delta p \\ \Delta r \\ \Delta\phi \end{bmatrix}$$

The eigenvalues can be determined by finding the eigenvalues of the matrix **A**:

$$|\lambda\mathbf{I} - \mathbf{A}| = 0$$

**TABLE 5.2**
**Lateral derivatives for the general aviation airplane**

| | |
|---|---|
| $Y_v = -0.254\ (s^{-1})$ | $L_v = -0.091\ (ft \cdot s)^{-1}$ |
| $Y_\beta = -45.72\ (ft/s^2)$ | $L_\beta = -16.02\ (s^{-2})$ |
| $Y_p = 0$ | $L_p = -8.4\ (s^{-1})$ |
| $Y_r = 0$ | $L_r = 2.19\ (s^{-1})$ |
| $N_v = 0.025\ (ft \cdot s)^{-1}$ | |
| $N_\beta = 4.49\ (s^{-2})$ | |
| $N_p = -0.35\ (s^{-1})$ | |
| $N_r = -0.76\ (s^{-1})$ | |

The resulting characteristic equation is

$$\lambda^4 + 9.417\lambda^3 + 13.982\lambda^2 + 48.102\lambda + 0.4205 = 0$$

Solution of the characteristic equation yields the lateral eigenvalues:

$\lambda = -0.00877$ (Spiral mode)

$\lambda = -8.435$ (Roll mode)

$\lambda = -0.487 \pm i(2.335)$ (Dutch roll mode)

The estimates for the lateral eigenvalues using the approximate expressions is obtained as follows:

$$\lambda_{spiral} = \frac{L_\beta N_r - L_r N_\beta}{L_\beta}$$

Susbtituting in the numerical values for the derivatives yields

$$\lambda_{spiral} = [(-16.02\ s^{-2})(-0.76\ s^{-1}) - (2.19\ s^{-1})(4.49\ s^{-2})]/(-16.02\ s^{-2})$$
$$= -0.144\ s^{-1}$$
$$\lambda_{roll} = L_p = -8.4\ s^{-1}$$

The Dutch roll roots are determined from the characteristic equation given by Equation (5.44):

$$\lambda^2 - \frac{(Y_\beta + u_0 N_r)}{u_0}\lambda + \frac{Y_\beta N_r - N_\beta Y_r + u_0 N_\beta}{u_0} = 0$$

or

$$\lambda^2 + 1.102\lambda + 4.71 = 0$$

which yields the following roots

$$\lambda_{DR} = -0.51 \pm 2.109i$$

and

$$\omega_{n\,DR} = 2.17\ rad/s$$
$$\zeta_{DR} = 0.254$$



**TABLE 5.3**
**Comparison of exact and approximate roots**

| | Exact | | | Approximate | | |
|---|---|---|---|---|---|---|
| | $T_{1/2}$, s | $T_2$, s | $P$, s | $T_{1/2}$, s | $T_2$, s | $P$, s |
| Spiral | 78.7 | — | — | 4.79 | — | — |
| Roll | 0.082 | — | — | 0.082 | — | — |
| Dutch roll | 1.42 | — | 2.69 | 1.35 | — | 2.98 |

Table 5.3 compares the results of the exact and approximate analysis. For this example, the roll and Dutch roll roots are in good agreement. On the other hand, the spiral root approximation is very poor.

The relationship between good spiral and Dutch roll characteristics presents a challenge to the airplane designer. In Chapter 2 it was stated that an airplane should possess static stability in both the directional and roll modes. This implies the $C_{n_\beta} > 0$ and $C_{l_\beta} < 0$. However, if we examine the influence of these stability coefficients on the lateral roots by means of a root locus plot, we observe the following. As the dihedral effect is increased, that is, $C_{l_\beta}$ becomes more negative, the Dutch roll root moves toward the right half-plane, which means the Dutch roll root is becoming less stable and the spiral root is moving in the direction of increased stability. These observations are clearly shown in Figures 5.14 and 5.15.

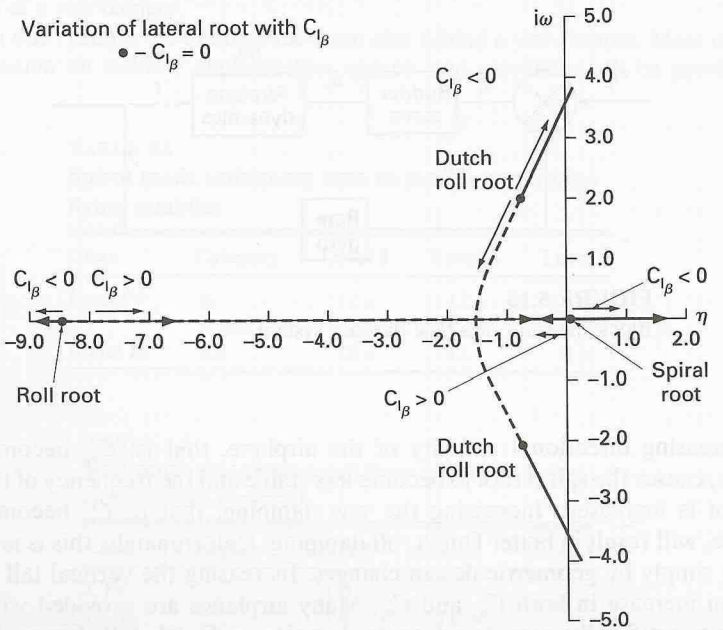


**FIGURE 5.14**
Variation of lateral roots with $C_{l_\beta}$.

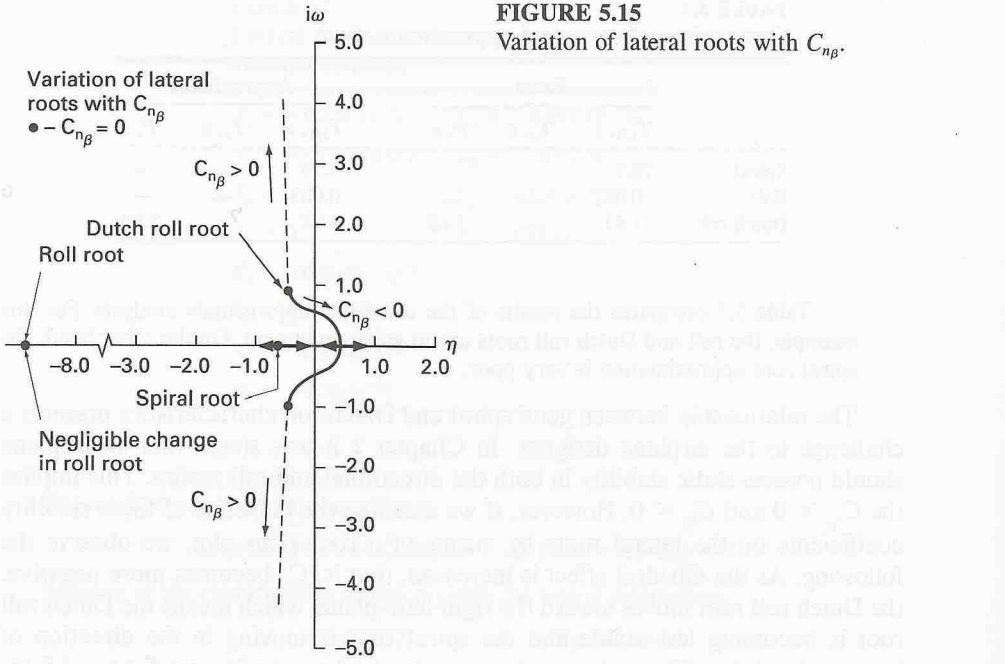


**FIGURE 5.15**
Variation of lateral roots with $C_{n_\beta}$.

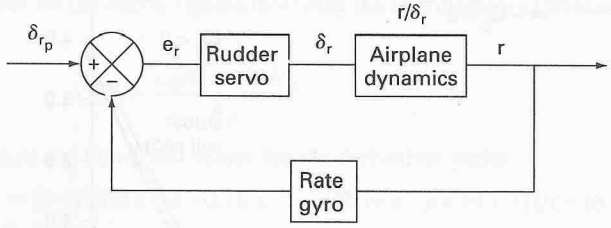


**FIGURE 5.16**
Block diagram of a yaw damper system.

Increasing directional stability of the airplane, that is, $C_{n_\beta}$ becomes more positive, causes the spiral root to become less stable and the frequency of the Dutch roll root is increased. Increasing the yaw damping, that is, $C_{n_r}$ becomes more negative, will result in better Dutch roll damping. Unfortunately, this is not easy to achieve simply by geometric design changes. Increasing the vertical tail size will cause an increase in both $C_{n_\beta}$ and $C_{n_r}$. Many airplanes are provided with a rate damper to artificially provide adequate damping in Dutch roll. Figure 5.16 is a sketch of a simple control system to provide increased yaw damping for the airplane.



## 5.5 LATERAL FLYING QUALITIES

In this chapter we examined the lateral direction characteristics of an airplane. The relationship between the aerodynamic stability and control derivatives and the lateral response was discussed. We have developed the necessary equations and analysis procedures to calculate the lateral dynamics. Although these techniques allow us to determine whether an airplane design is stable or unstable, by itself the analysis does not tell us whether the pilot will judge the airplane to have acceptable flying characteristics. To determine this the designer needs to know what dynamic characteristics are considered favorable by the pilots who will fly the airplane. This information is available through the lateral-directional flying quality specifications.

The lateral-directional flying quality requirements are listed in Tables 5.4, 5.5, and 5.6. The definition of class and category were presented in Chapter 4. In Example Problem 5.2 the aircraft would be considered a Class 1 vehicle and the flight phase as Category B. Using the information from Table 5.4, we find that the aircraft studied here has Level 1 flying qualities.

**EXAMPLE PROBLEM 5.4.** As shown earlier, the Dutch roll motion can be improved by increasing the magnitude of the yaw damping term $N_r$. One means of increasing $N_r$ is by increasing the vertical tail area. Unfortunately, increasing the vertical tail area will add additional drag to the airplane as well as increase the directional stability. The increase in directional stability will degrade the spiral characteristics of the airplane. For most transport and fighter aircraft, increased damping is provided artificially by means of a yaw damper.

In this example we examine the basic idea behind a yaw damper. More detailed information on stability augmentation systems and autopilots will be provided in

**TABLE 5.4**
**Spiral mode (minimum time to double amplitude) flying qualities**

| Class | Category | Level 1 | Level 2 | Level 3 |
|---|---|---|---|---|
| I and IV | A | 12 s | 12 s | 4 s |
| | B and C | 20 s | 12 s | 4 s |
| II and III | All | 20 s | 12 s | 4 s |

**TABLE 5.5**
**Roll mode (maximum roll time constant) flying qualities (in seconds)**

| Class | Category | Level 1 | Level 2 | Level 3 |
|---|---|---|---|---|
| I, IV | A | 1.0 | 1.4 | 10 |
| II, III | | 1.4 | 3.0 | |
| All | B | 1.4 | 3.0 | 10 |
| I, IV | C | 1.0 | 1.4 | 10 |
| II, III | | 1.4 | 3.0 | |

TABLE 5.6
**Dutch roll flying qualities**

| Level | Category | Class | Min $\zeta$* | Min $\zeta\omega_n$,* rad/s | Min $\omega_n$, rad/s |
|---|---|---|---|---|---|
| 1 | A | I, IV | 0.19 | 0.35 | 1.0 |
| | | II, III | 0.19 | 0.35 | 0.4 |
| | B | All | 0.08 | 0.15 | 0.4 |
| | C | I, II-*C* IV | 0.08 | 0.15 | 1.0 |
| | | II-*L*, III | 0.08 | 0.15 | 0.4 |
| 2 | All | All | 0.02 | 0.05 | 0.4 |
| 3 | All | All | 0.02 | — | 0.4 |

Where *C* and *L* denote carrier- or land-based aircraft.
*The governing damping requirement is that yielding the larger value of $\zeta$.

Chapters 7–10. To examine how a yaw damper can be used to provide damping for an airplane, consider the yawing moment equation developed earlier:

$$\Delta\ddot{\psi} - N_r\,\Delta\dot{\psi} + N_\beta\,\Delta\psi = N_{\delta_r}\,\Delta\delta_r$$

Suppose that for a particular airplane the static directional stability, yaw damping, and control derivatives were as follows:

$$N_\beta = 1.77\ \text{s}^{-2} \qquad N_r = -0.10\ \text{s}^{-1} \qquad N_{\delta_r} = -0.84\ \text{s}^{-1}$$

For this airplane the damping ratio and undamped natural frequency would be

$$\zeta = -\frac{N_r}{2\sqrt{N_\beta}} = 0.037 \qquad \omega_n = \sqrt{N_\beta} = 1.33\ \text{rad/s}$$

The low damping ratio would result in a free response that would have a large overshoot and poor damping. Such an airplane would be very difficult for the pilot to fly. However, we could design a feedback control system such that the rudder deflection is proportional to the yaw rate; that is,

$$\Delta\delta_r = -k\,\Delta\dot{\psi}$$

Substituting the control deflection expression into the equation of motion and rearranging yields

$$\Delta\ddot{\psi} - (N_r - kN_{\delta_r})\,\Delta\dot{\psi} + N_\beta\,\Delta\psi = 0$$

By proper selection of $k$ we can provide the airplane whatever damping characteristics we desire. For the purpose of this example, consider the simple yawing motion to be an approximation of the Dutch roll motion. The flying quality specifications included in Table 5.6 state that a Level 1 flying quality rating would be achieved for the landing flight phase if

$$\zeta > 0.08 \qquad \zeta\omega_n > 0.15\ \text{rad/s} \qquad \omega_n > 0.4\ \text{rad/s}$$

A damping ratio of 0.2 and a frequency of 1.33 would be considered acceptable by pilots. The problem now is to select the unknown gain $k$ so that the airplane has the desired damping characteristics. If we compare the yaw moment equation of motion to the standard form for a second-order system, we can establish a relationship for $k$ as follows:

$$2\zeta\omega_n = -(N_r - kN_{\delta_r}) \qquad 0.532 = -[-0.1 - k(-0.84)] \qquad k = -0.514$$

Figure 5.16 is a sketch of a simple yaw damper stability augmentation system.

Although we designed a feedback system to provide improved damping, it is possible to control both the damping and the frequency. This can be accomplished by making the rudder deflection proportional to both the yaw rate and yaw angle; that is,

$$\Delta\delta_r = -k_1\,\Delta\dot{\psi} - k_2\,\Delta\psi$$

Substituting this expression back into the differential equation yields

$$\Delta\ddot{\psi} - (N_r - k_1N_{\delta_r})\,\Delta\dot{\psi} + (N_\beta + k_2)\,\Delta\psi = 0$$

The gains $k_1$ and $k_2$ then are selected so that the characteristic equation has the desired damping ratio and frequency. The use of feedback control to augment the stability characteristics of an airplane plays an important role in the design of modern aircraft. By using stability augmentation systems, the designer can ensure good flying qualities over the entire flight regime. Furthermore, with the addition of a stability augmentation system, the designer can reduce the inherent aerodynamic static stability of the airplane by reducing the vertical tail size. Thus, the designer can achieve an improvement in performance without compromising the level of flying qualities.



## 5.6 INERTIAL COUPLING

In the analysis presented in this and the previous chapter, we treated the longitudinal and lateral equations separately. In so doing we assumed that there is no coupling between the equations. However, slender high-performance fighter aircraft can experience significant roll coupling that can result in divergence from the desired flight path, causing loss of control or structural failure.

The mechanisms that cause this undesirable behavior can be due to inertial or aerodynamic coupling of the equations of motion. To explain how inertial coupling occurs, we examine the nonlinearized moment equations developed in Chapter 3. The moment equations are reproduced in Equation (5.49):

$$\begin{aligned}
\textstyle\sum \text{Roll moments} &= I_x\dot{p} + qr(I_z - I_y) - (\dot{r} + qp)I_{xz} \\
\textstyle\sum \text{Pitching moments} &= I_y\dot{q} + pr(I_x - I_z) + (p^2 - r^2)I_{xz} \qquad (5.49) \\
\textstyle\sum \text{Yawing moments} &= I_z\dot{r} + pq(I_y - I_x) + (qr - \dot{p})I_{xz}
\end{aligned}$$

The first cases of inertial coupling started to appear when fighter aircraft designs were developed for supersonic flight. These aircraft were designed with

low aspect ratio wings and long, slender fuselages. In these designs, more of the aircraft's weight was concentrated in the fuselage than in the earlier subsonic fighters. With the weight concentrated in the fuselage, the moments of inertia around the pitch angle yaw axis increased and the inertia around the roll axis decreased in comparison with subsonic fighter aircraft.

On examining Equation (5.49) we see that the second term in the pitch equation could be significant if the difference in the moments of inertia becomes large. For the case of a slender high-performance fighter executing a rapid rolling maneuver the term $pr(I_x - I_z)$ can become large enough to produce an uncontrollable pitching motion.

A similar argument can be made for the product of inertia terms in the equations of motion. The product of inertia $I_{xz}$ is a measure of the uniformity of the distribution of mass about the $x$ axis. For modern fighter aircraft $I_{xz}$ typically is not 0. Again we see that if the airplane is executing a rapid roll maneuver the term $(p^2 - r^2)I_{xz}$ may be as significant as the other terms in the equation.

Finally, aerodynamic coupling also must be considered when aircraft are maneuvering at high angular rates or at high angles of attack. As was discussed in Chapter 4 high angle of attack flow asymmetries can cause out-of-plane forces and moments even for symmetric flight conditions. Such forces and moments couple the longitudinal and lateral equations of motion.

## 5.7 SUMMARY

In this chapter we examined the lateral modes of motion. The Dutch roll and spiral motions were shown to be influenced by static directional stability and dihedral effect in an opposing manner. The designer is faced with the dilemma of trying to satisfy the flying quality specifications for both the spiral and Dutch roll modes. This becomes particularly difficult for airplanes that have extended flight envelopes. One way designers have solved this problem is by incorporating a yaw damper in the design. The yaw damper is an automatic system that artificially improves the system damping. The increased damping provided by the yaw damper improves both the spiral and Dutch roll characteristics.

## PROBLEMS

Problems that require the use of a computer have a capital C after the problem number.

**5.1.** Determine the response of the A-4D to a 5° step change in aileron deflection. Plot the roll rate versus time. Assume sea-level standard conditions and that the airplane is flying at $M = 0.4$. What is the steady-state roll rate and time constant for this motion?



**5.2.** For the roll response shown in Figure P5.2, estimate the aileron control power $L_{\delta_a}$ and the roll damping derivative $L_p$. Information on the characteristics of the airplane is in the figure.

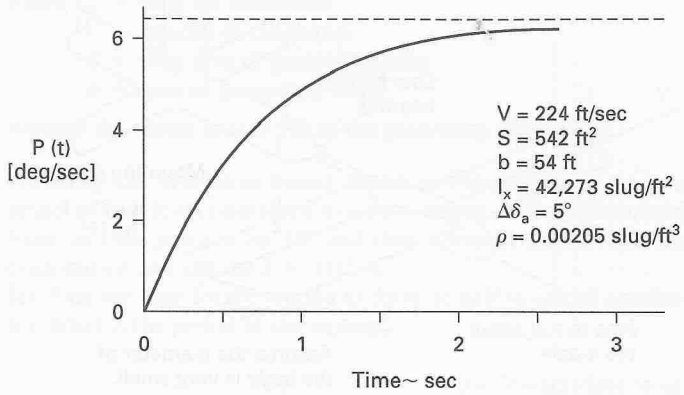


**FIGURE P5.2**
Roll rate time history.

**5.3.** A wind-tunnel model free to rotate about its $x$ axis is spun up to 10.5 rad/s by means of a motor drive system. When the motor drive is disengaged, the model spin will decay as shown in Figure P5.3. From the spin time history determine the roll damping derivative $L_p$.

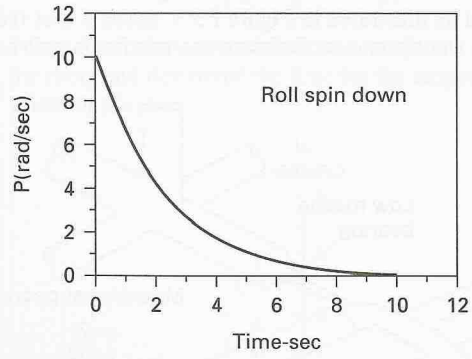


**FIGURE P5.3**
Roll rate time history.

**5.4.** A wind-tunnel model is constructed of two small lifting surfaces mounted to an axisymmetric body as illustrated in Figure P5.4. The body houses a set of ball bearings that permit the model to roll freely about the longitudinal or $x$ axis. The right lifting surface (positive $y$ axis) is mounted to the body at a $-3°$ and the left lifting surface is set at a $+3°$.

(*a*) Estimate the rolling moment of inertia, $I_x$, of the model. Approximate the lifting surfaces as thin flat plates. Neglect the body contribution.

(*b*) Estimate the roll torque due to the differential mounting incidence. Express your answer as a roll moment coefficient per unit deflection, $C_{l_\delta}$.

(*c*) Estimate the roll damping coefficient, $C_{l_p}$.

(*d*) Calculate the response of the model if it is released from the rest. Neglect the friction of the bearings.

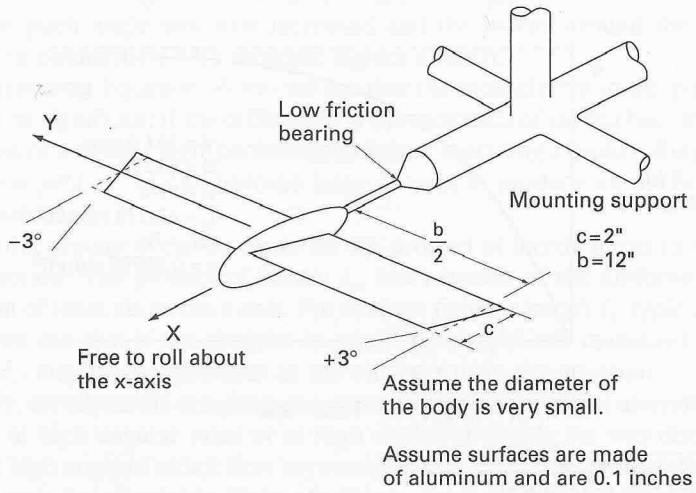


**FIGURE P5.4**

**5.5.** Suppose the wing segments for the model described in Problem 5.4 are set so that there is no differential incidence between the two sections. If the wings are mounted in this manner, the roll torque due to the differential incidences will be 0. Now consider what would happen if a half-span wing were mounted upstream of the free-to-roll model as illustrated in Figure P5.5. Assume that the free-to-roll wing is centered in the tip vortex. Estimate the maximum roll rate of the

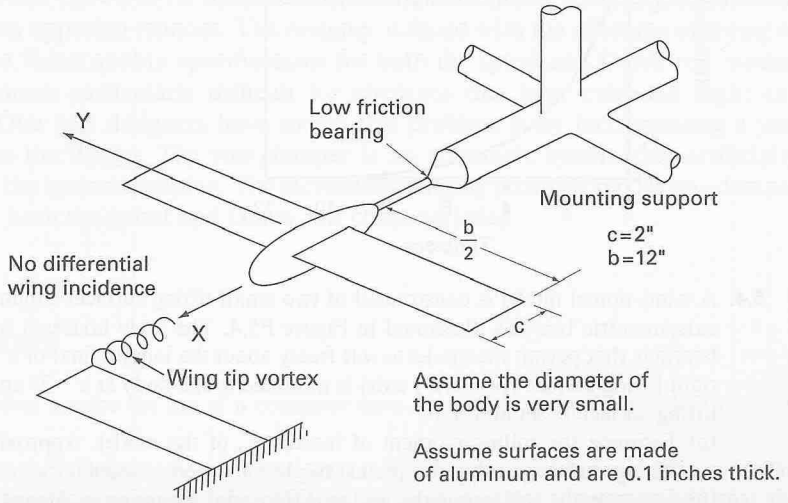


**FIGURE P5.5**



free-to-roll wing. The strength of the vortex can be shown to be as follows.

$$\Gamma = \frac{8C_L VS}{\pi b}$$

where $C_L$ = wing lift coefficient
$V$ = velocity of the tunnel
$S$ = wing area of generating wing
$b$ = span of generating wing.

Assume the vortex core is 5% of the generating wing span.

**5.6.** Assuming the cruciform finned model in Figure P5.6 is mounted in a wind tunnel so that it is constrained to a pure yawing motion. The model is displaced from its trim position by 10° and then released. Neglect the fuselage and $\dot{\beta}$ contribution and assume $S = \pi D^2/4$.
(*a*) Find the time for the motion to damp to half its initial amplitude.
(*b*) What is the period of the motion?

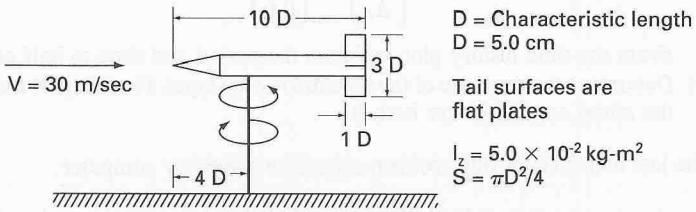


**FIGURE P5.6**
Yawing wind-tunnel model.

**5.7.** Figure P5.7. shows the stick fixed lateral roots of a jet transport airplane. Identify the roots and determine the time for the amplitude and period to halve or double where applicable.

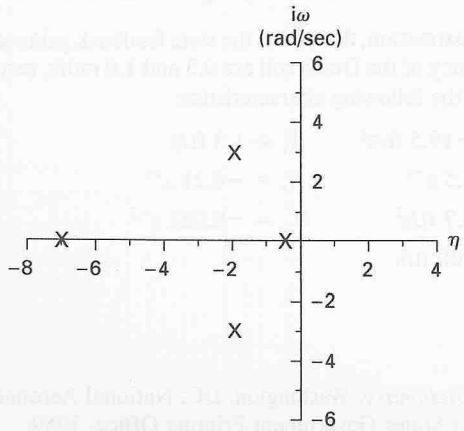


**FIGURE P5.7**
Lateral roots for a jet transport.

**5.8(C).** The Dutch roll motion can be approximated using the following equations:

$$\begin{bmatrix} \Delta\dot{\beta} \\ \Delta\dot{r} \end{bmatrix} = \begin{bmatrix} \frac{Y_\beta}{u_0} & -\left(1 - \frac{Y_r}{u_0}\right) \\ N_\beta & N_r \end{bmatrix} \begin{bmatrix} \Delta\beta \\ \Delta_r \end{bmatrix} + \begin{bmatrix} \frac{Y_{\delta_r}}{u_0} \\ N_{\delta_r} \end{bmatrix} \Delta\delta_r$$

Assume the coefficients in the plant matrix have the following numerical values:

$$Y_\beta = -7.8 \text{ ft/s}^2 \qquad N_r = -0.34 \text{ 1/s} \qquad Y_{\delta_r} = -5.236 \text{ ft/s}^2$$
$$Y_r = 2.47 \text{ ft/s} \qquad u_0 = 154 \text{ ft/s} \qquad N_{\delta_r} = 0.616 \text{ 1/s}^2$$
$$N_\beta = 0.64 \text{ 1/s}^2$$

(*a*) Determine the Dutch roll eigenvalues.
(*b*) What is the damping ratio and undamped natural frequency?
(*c*) What is the period and time to half amplitude of the motion?
(*d*) Determine the response of the system if the initial conditions are as follows:

$$\begin{bmatrix} \Delta\beta \\ \Delta r \end{bmatrix} = \begin{bmatrix} 0.1 \\ 0.0 \end{bmatrix}$$

From the time history plot, estimate the period and time to half amplitude.
(*e*) Determine the response of the system to a step input. For this part assume that the initial conditions are both 0.

The last two parts of this problem should be solved by computer.

**5.9(C).** Develop a computer code to obtain the stick fixed lateral eigenvalues from the lateral stability matrix. Use your computer program to analyze the lateral motion of the 747 jet transport. Estimated aerodynamic, mass, and geometric characteristics of the 747 are included in Appendix B. The MATLAB Software is suggested for this problem.

**5.10(C).** Using the program developed in problem 5.9, examine the influence of $C_{l_\beta}$ and $C_{n_r}$ on the lateral roots. Use the 747 data, but vary $C_{l_\beta}$ and $C_{n_r}$ separately.

**5.11.** Using the Dutch roll approximation, determine the state feedback gains so that the damping ratio and frequency of the Dutch roll are 0.3 and 1.0 rad/s, respectively. Assume the airplane has the following characteristics:

$$Y_\beta = -19.5 \text{ ft/s}^2 \qquad Y_r = 1.3 \text{ ft/s}$$
$$N_\beta = 1.5 \text{ s}^{-2} \qquad N_r = -0.21 \text{ s}^{-1}$$
$$Y_{\delta_r} = 4.7 \text{ ft/s}^2 \qquad N_{\delta_r} = -0.082 \text{ s}^{-2}$$
$$u_0 = 400 \text{ ft/s}$$

## REFERENCES


5.1. Adams, F. D. *Aeronautical Dictionary*. Washington, DC: National Aeronautics and Space Administration, United States Government Printing Office, 1959.
5.2. Arena, A. S., Jr.; and R. C. Nelson. "Experimental Investigations on Limit Cycle Wing Rock of Slender Wings." AIAA Journal of Aircraft 31, no. 5 (September–October 1994) pp. 1148–1155.





5.3. Arena, A. S., Jr.; R. C. Nelson; and L. B. Schiff. "An Experimental Study of the Nonlinear Dynamic Phenomenon Known as Wing Rock." AIAA Paper No. 60–2813, August 1990.
5.4. Seckel, E. *Stability and Control of Airplanes and Helicopters*. New York: Academic Press, 1964.
5.5. Etkin, B. *Dynamics of Flight*. New York: Wiley, 1972.
5.6. Hage, R. E.; and C. D. Perkins. *Airplane Performance, Stability and Control*. New York: Wiley, 1949.
5.7. Roskam, J. *Flight Dynamics of Rigid and Elastic Airplanes*. Lawrence: University of Kansas Press, 1972.
5.8. Fung, Y. C. *The Theory of Aeroelasticity*. New York: Wiley, 1955.
5.9. Bisplinghoff, R. L.; H. Ashley; and R. L. Halfman. *Aeroelasticity*. Reading, MA: Addison Wesley, 1955.
5.10. Scanlan, R. H.; and R. Rosenbaum. *Introduction to the Study of Aircraft Vibration and Flutter*. New York: Macmillan, 1951.
5.11. Abramson, H. *The Dynamics of Airplanes*. New York: Ronald Press, 1958.